Angle-resolved constant-initial-state spectroscopy of GaAs

J. Fraxedas
Max-Planck-Institut für Festkörperforschung, Heisenbergstrasse 1, D-7000 Stuttgart 80, Federal Republic of Germany

A. Stampfl, R. C. G. Leckey, and J. D. Riley
Department of Physics, La Trobe University, Bundoora, Victoria 3083, Australia

L. Ley
Institut für Technische Physik, Universität Erlangen-Nürnberg, D-8520 Erlangen, Federal Republic of Germany

(Received 14 May 1990)

The conduction-band energies at the Γ point of GaAs are determined experimentally in the 10–60-eV range by means of angle-resolved constant-initial-state measurements. The most prominent conduction-band states reached from the top (Γ_{15}^{v}) and the bottom (Γ_{1}^{v}) of the valence band lie at 10.72, 12.60, 15.20, 22.62, 32.38, 34.13, 35.61, 49.43, 55.67, and 58.61 eV above the valence-band maximum, respectively. These values are compared with available theoretical conduction-band calculations. We observe resonant photoemission at 20.30 eV, which corresponds to the transition from the Ga 3*d* surface core level to the unoccupied Ga-derived dangling bond. Associated with this transition is a surface exciton with a binding energy of approximately 0.93 eV. We observe also a weak but reproducible resonance at 106.40 eV, which is associated with the transition from the Ga 3*p* core to the same unoccupied band. A further resonance at 43.86 eV is assigned to the excitation of the As 3*d* core level into the bulk conduction band. The contribution of intra- as well as interatomic Auger processes and of inelastic scattering due to plasmon losses in the measured spectra is also considered.

I. INTRODUCTION

The experimental determination of the energies of unoccupied surface and bulk states in metals and semiconductors has made considerable progress in recent years. Ellipsometric measurements[1] as well as two-photon[2] and near-band-gap photoemission[3] experiments give the relative energies between initial- and final-state critical points up to approximately 5 eV above the valence-band maximum (VBM). The maximum energy reported for the conduction bands of GaAs at the Γ point is about 10 eV above the VBM measured by means of electroreflectance spectroscopy.[4] Recently, an ellipsometer working with synchrotron radiation has been developed[5] which will allow energy studies up to approximately 30 eV above the VBM.

The absorption threshold from the core levels to unoccupied states has been measured with photoemission yield spectroscopy[6] and by means of electron-energy-loss experiments.[7] Another technique is based on photoelectron spectroscopy of highly *n*-type-doped materials. In this case the pinning of the Fermi level above the conduction-band minimum allows a direct observation of the low-lying populated conduction bands.[8]

All these methods except the last measure transition energies in which electron-hole interaction is always present. The most direct method for the final-state band mapping is inverse photoemission.[9] In this case no electron-hole interaction is present since no hole is created; however, this technique still involves many-body effects.

The method that will be used in the present work is angle-resolved constant-initial-state (ARCIS) spectroscopy. Photoelectrons associated with direct transitions from an initial state with fixed energy ε_i are detected provided a final state is available. The measurements are performed by the simultaneous scanning of the photon energy $\hbar\omega$ and the kinetic energy K of the electrons such that the difference $\hbar\omega - K = \varepsilon_i + \Phi_T$ remains constant (Φ_T represents the photoelectric threshold). In this case many-body effects such as relaxation, electron-hole interaction, Auger processes, etc., are present. This method was introduced by Lapeyre and co-workers[10] and has been used for the experimental determination of the energy position and symmetry of the conduction bands,[11,12] for the location of excitonic states above the VBM,[13] and for the study of impurity-induced levels in semiconductors,[14] to mention a few applications. The results can be used to examine the energy range for which the final states can be considered as free-electron-like. This is of interest from a theoretical point of view as well as for the interpretation of angle-resolved photoemission (ARPES) data, which are usually made assuming free-electron final states. The example of graphite shows, however, the influence of the crystal potential for energies as high as 90 eV above the VBM.[11]

As mentioned above, the initial-state energy is chosen experimentally, but the location of the initial state in **k** space depends on available direct transitions. It must therefore be inferred with the help of band-structure calculations. This last point does not represent a limitation in the present case since the initial-state band structure of GaAs is well understood both theoretically and experimentally.

In the present study we have performed ARCIS on GaAs for final-state energies in the 10–60 eV range. We have extended earlier ARCIS (Ref. 15) and electroreflectance work on GaAs,[4] for which the final-state energies were measured up to approximately 15 eV. The necessity of more-realistic final-state bands (beyond the free-electron approximation) has been claimed to explain the asymmetric line shape of critical point transitions in GaAs measured with angle-resolved photoemission.[16]

In Sec. II a short description of the experimental details is given, while Sec. III is devoted to the presentation of the experimental data and their analysis. Section IV contains the summary.

II. EXPERIMENTAL DETAILS

ARCIS measurements were performed at room temperature with a toroidal energy analyzer which collects simultaneously all polar angles from $-90°$ to $90°$.[17] The angular resolution is $\pm 1°$ and the combined analyzer-monochromator resolution is better than 0.25 eV. The base pressure in the measurement chamber was 1×10^{-10} mbar. Monochromatized light was delivered by a toroidal grating monochromator (TGM4) at the Synchrotron Radiation facility BESSY (Berlin).

For the experiments reported here special care was taken to obtain correct values of the photon energy. This was done by measuring the Ga $3d$ core levels simultaneously with first- and second-order light and obtaining the differences. The error in the monochromator setting was found to be less than 0.2 eV over the photon range 9–70 eV.

III. RESULTS

We have performed measurements on cleaved (110) faces of n-type doped GaAs ($n\sim10^{16}$ cm^{-3}) along the [001] azimuth. Our analysis was performed for the features identified in Fig. 1. In this figure we show the ARCIS spectra taken at normal emission for transitions arising from the VBM at Γ_{15}^{v} [Figs. 1(a) and 1(b)] and from the bottom of the valence bands at Γ_{1}^{v} [Fig. 1(c)] which lies 13.25 eV below the VBM. Photons in the 9–70-eV range were used. The measured, or apparent, photoelectron threshold ($\Phi'_T=4.25$ eV) depends on the work function of the spectrometer; the accepted value for the photoelectron threshold Φ_T of GaAs for the (110) surface is 5.56 eV (Ref. 18) and depends rather strongly on the surface quality. Peaks labeled E_0 correspond to the major features that are assigned to direct transitions arising from both Γ_{15}^{v} and Γ_{1}^{v}. (The inclusion of the shoulder E_0^V will be justified later.) Peaks labeled R refer

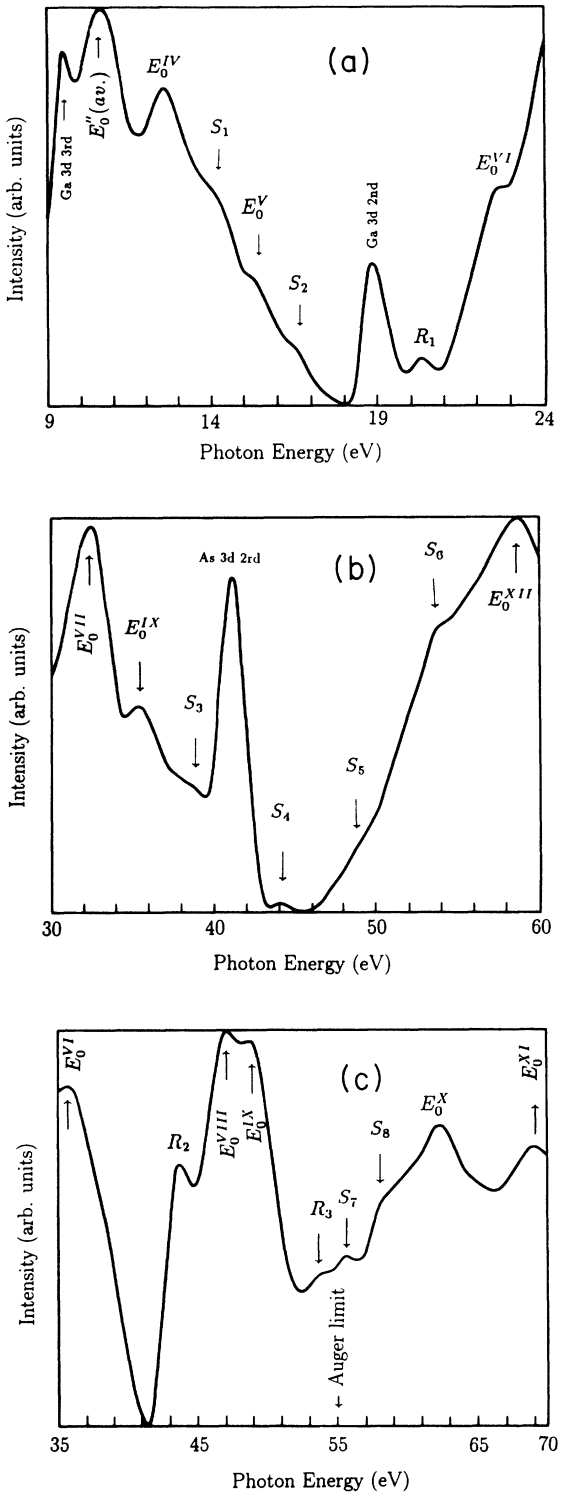

FIG. 1. Normal-emission constant-initial-state spectra of GaAs at the Γ point measured at room temperature. Features labeled E_0, R, and S are discussed in the text. Ga and As $3d$ core levels excited with second- and third-order light from the monochromator are indicated. (a) Initial state at $\varepsilon_i=0$ (Γ_{15}^{v}). The photon energy ranges from 9 to 24 eV. (b) Initial state at $\varepsilon_i=0$ (Γ_{15}^{v}). The photon energy ranges from 30 to 60 eV. (c) Initial state at $\varepsilon_i=13.25$ eV below the VBM (Γ_{1}^{v}). The photon energy ranges from 35 to 70 eV. The Auger limit associated with the As $3d$ core levels is also shown.

to resonances and S to less prominent features. Finally, the Ga $3d$ and As $3d$ core levels excited with second- and third-order light from the monochromator are also identified in Fig. 1.

Our analysis concentrates on these normal-emission data. Further work on off-normal emission is planned to be published in a future contribution.[19] Furthermore, the main results of this work are related to the Γ point. Here the analysis is less ambiguous since the different energy gaps in the conduction band are large (about 5 eV) because Γ has the full space-group symmetry. Results from the X point will also be discussed, but due to its lower symmetry the band gaps are smaller and, as a consequence, the analysis becomes very complex. However, a study of the energies at X is necessary because surface umklapp processes may be present.

Figure 2 presents normal-emission data for different ε_i along the Σ symmetry line in $\mathbf{k}$ space. In Figs. 2(a) and 2(b) the ARCIS spectra from Γ_{15}^v to X_3^v (6.50 eV below the VBM) and from X_1^v (10.25 eV below the VBM) to Γ_1^v (13.25 eV below the VBM), respectively, are shown.

Before proceeding with the detailed analysis of the spectra, we discuss the geometry used in this experiment and the influence that surface states may have on the data. The sample is oriented with the natural cleavage face (110) at 45° from the incident monochromatized synchrotron light. The photons are p-polarized in the plane spanned by the [110] and [001] directions of the sample axis. In the chosen geometry, the Ga dangling bond is nearly perpendicular to the polarization vector $\hat{a}$ so that its contribution will be strongly reduced, whereas we expect to observe an enhancement of the As dangling-bond-related features since $\hat{a}$ is nearly parallel to it. The increase in intensity for the As-derived surface states could introduce, in principle, difficulties in our analysis from the Γ_{15}^v point. According to theoretical calculations of the relaxed GaAs(110) surface,[20] there is a surface resonance immediately below the VBM with a position that depends on the surface quality.[21] The linewidth of the dangling-bond-derived surface peak is of the order of 0.3 eV for GaAs, a value that arises mostly from the distortion of the dangling bonds due to steps at the surface, which to some extent are always present. This point has been discussed in more detail in Ref. 22. A contribution from this resonance might thus be expected in an ARCIS spectrum with $\varepsilon_i = 0$.

Because surface states and surface resonances have no dispersion along the perpendicular component of the wave vector k_z, the transition probability is proportional to the one-dimensional (along k_z) density of conduction states along Γ-K-X. In order to estimate the actual influence of the surface resonance near Γ_{15}^v to the spectra of Figs. 1 and 2, we have tried to identify singularities in the one-dimensional density of states along Γ-K-X. To this end we analyze the ARCIS spectra from just below $\Sigma_1^{\min}$ (4.00 eV below the VBM) to X_3^v (6.50 eV below the VBM) where no surface states or resonances are present at $\bar{\Gamma}$.[20,23] In this energy region where only transitions from one initial-state band contribute to the ARCIS spectra, we obtain for every value of ε_i a unique k_z by using the theoretical initial states of Ref. 24. Direct transitions

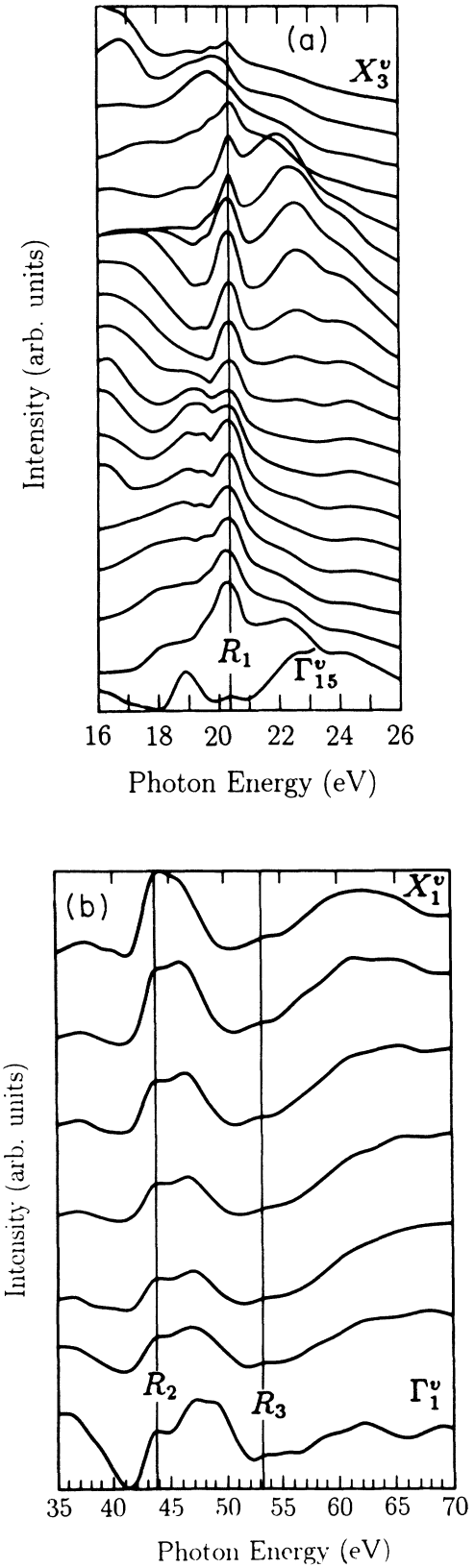

FIG. 2. Normal-emission constant-initial-state spectra as a function of the initial-state energy ε_i. Resonances R_1, R_2, and R_3 are identified. (a) From $\varepsilon_i = 0$ (Γ_{15}^v) to $\varepsilon_i = 6.50$ eV below the VBM (X_3^v). (b) From $\varepsilon_i = 10.25$ eV below the VBM (X_1^v) to $\varepsilon_i = 13.25$ eV below the VBM (Γ_1^v) in steps of 0.5 eV.

from these points allow us to make a comparison with the theoretical final-state band structure. As shown in Fig. 3, the experimental final-state energies follow the band in the region 10 eV above the VBM resonably well and the critical point (maximum) in the final-state band dispersion at approximately 12 eV is reproduced. This critical point leads to a singularity in the one-dimensional density of final states and is therefore expected to show up in the ARCIS spectra if the surface resonance at Γ would make a significant contribution to the spectra of Figs. 1 and 2. The corresponding feature would fall between peaks E_0'' (av) and E_0^{IV} and is not observed in our data [see Fig. 1(a)].

Additional evidence for the fact that the spectra of Figs. 1 and 2 are not dominated by surface states comes from the widths of the spectral features. The widths of the peaks in Fig. 1 are of the order of 2 to 4 eV, values that are typical of the final-state inverse lifetimes due to electron inelastic scattering. This observation can be easily understood on the basis of direct transitions arising from the top of the dispersing bulk valence band at Γ_{15}^v and if the inverse lifetime of the hole created at Γ_{15}^v is negligible compared to the final-state inverse lifetime. If a nondispersing state at the VBM were responsible, then only the density of the final states would be measured, which is almost structureless at higher energies. We observe, however, clear structures which imply that the spectra are mainly due to direct, k_z-conserving transitions arising from the bulk band at Γ_{15}^v. Of course, the presence of surface resonances cannot be completely ruled out.

The dispersion of final-state bands can also be determined with conventional ARPES by assuming direct transitions from initial states with a known dispersion,[25,26] assumptions also adopted in our ARCIS analysis. References 25 and 26 report conduction-band points up to approximately 20 eV but none of them report data at the Γ point, because of the ambiguity associated with the determination of the VBM.[27] ARCIS is a more systematic method of studying unoccupied states because ε_i can be fixed so that only transitions from the intersection of the line $\varepsilon_i = \text{const}$ with $\varepsilon_i(\mathbf{k})$ are possible. The exact determination of the ε_i values associated with Γ_{15}^v, Γ_1^v, X_3^v, and X_1^v can be performed accurately because no valence-band emission is observed for values of ε_i in the forbidden gaps ($\varepsilon_i < 0$, $6.50 < \varepsilon_i < 10.25$ eV, and $\varepsilon_i > 13.25$ eV). We thus reach these critical points by varying ε_i in small energy steps (0.12 eV) until valence-band emission is observed.

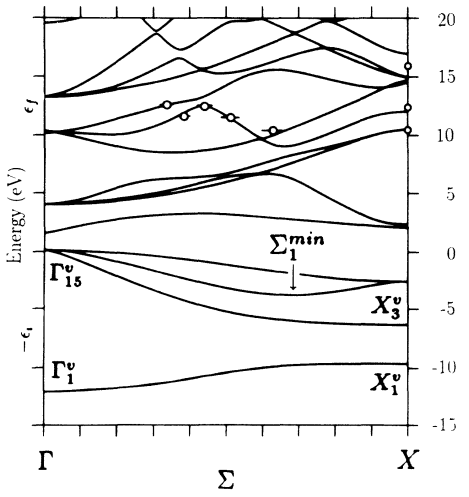

FIG. 3. Band structure of GaAs along Γ-K-X from Ref. 30. Points correspond to direct transitions arising from the initial band from just below Σ_1^{min} ($\varepsilon_i = 4.00$ eV below the VBM) to X_3^v ($\varepsilon_i = 6.50$ below the VBM). Also shown is the uncertainty in k_z which increases as one approaches X_3^v due to the loss of dispersion in the initial-state band.

A. E_0 transitions

In Table I we show the energies, referred to the VBM, of features labeled E_0 in Fig. 1. Together with our experimental results, we list electroreflectance data from Refs. 28, 4, and from prior ARCIS results on GaAs.[15] E_0(av) represents the average value for the transitions E_0 ($\Gamma_8^v \rightarrow \Gamma_6^c$) and $E_0 + \Delta_0$ ($\Gamma_7^v \rightarrow \Gamma_6^c$), where Δ_0 is the spin-orbit splitting at the VBM. In our case, E_0(av), the fundamental gap, accounts for the transition $\Gamma_{15}^v \rightarrow \Gamma_1^c$, i.e., neglecting the spin-orbit splitting at the Γ point which is not resolved in our experiment. Features E_0'(av), E_0''(av), and E_0'''(av) follow the same criteria. E_0'(av) accounts for the $\Gamma_{15}^v \rightarrow \Gamma_{15}^c$ transition, E_0'''(av) for the $\Gamma_{15}^v \rightarrow \Gamma_1^c$, and E_0''(av) for the $\Gamma_{15}^v \rightarrow \Gamma_{12}^c$. New data, relating to features at higher energies, are labeled with roman superscripts (E_0^{IV}, E_0^{V}, etc.). Where values are obtained with more than one method, the scatter in energies is seen to lie within the experimental uncertainty of our data (± 0.1 eV).

TABLE I. Conduction-band energies at the Γ point relative to the VBM. E_0(av) is the fundamental gap. Our data complete earlier work on electroreflectance (Refs. 28 and 4) and on ARCIS (Ref. 15) up to approximately 60 eV. The temperature at which the measurements were performed is also shown.

in eV	$T = 4.2$ K[a] $T = 80$ K[b]	$T = 300$ K[c]	$T = 300$ K[d]
E_0(av)	1.632 ($T = 4.2$ K)		
E_0'(av)	4.716 ($T = 4.2$ K)		
E_0'''(av)	8.33 ($T = 80$ K)		
E_0''(av)	10.53 ($T = 80$ K)	10.6	10.72
E_0^{IV}		12.8	12.60
E_0^{V}		14.9	15.20
E_0^{VI}			22.62
E_0^{VII}			32.38
E_0^{VIII}			34.13
E_0^{IX}			35.61
E_0^{X}			49.43
E_0^{XI}			55.67
E_0^{XII}			58.61

[a]Reference 28.
[b]Reference 4.
[c]Reference 15.
[d]This work.

Next, we compare the experimental critical point energies with theoretical conduction-band calculations from Refs. 29 and 30. This comparison is shown in Fig. 4 for final-state energies up to 50 eV above the VBM.

The theoretical predictions of Ref. 30 are based on the *ab initio* self-consistent fully relativistic linear muffin-tin-orbital (LMTO) method.[24] The $\Gamma_{15}^{v}\rightarrow\Gamma_{1}^{c}$ band gap has been adjusted to correct for deficiencies in the use of local-density functionals which make the calculation inadequate for energies far from the fundamental gap. The reason to compare our results with these theoretical predictions is to test in which energy range the model is valid. As has been shown in Ref. 16, transitions arising from the L point (6.62 eV below the VBM) up to 14.6 eV above the VBM in GaAs are well predicted by this model. In our present work we use the nonrelativistic bands to simplify the analysis.[30] The theoretical predictions of Ref. 29 are based on self-consistent LMTO calculations and are a generalization of the work performed in Ref. 31. In a future study, we will present a comparison of the experimental data with available empirical-pseudopotential-method (EPM) calculations[32] (up to 28 eV above the VBM) and our own calculations up to 60 eV above the VBM,[33] where the symmetry of the states and their orbital character will also be analyzed.

For the E_0''(av) feature, we observe good agreement between the three different experiments referred to in Table I and also good agreement with the theoretical predictions considered here (see Fig. 4). Furthermore, both ARCIS experiments agree on the energy of E_0^{IV}. In this case the predicted energy from Ref. 30 lies closer to E_0^{IV} than the corresponding one from Ref. 29. The first noticeable discrepancy between both calculations is found in the next band. Reference 30 predicts a band at about 20 eV above the VBM and Ref. 29 at about 15 eV. The corresponding transition is observed in Ref. 15 as a peak and in the present work as a shoulder. In our case this feature appears obscured by the shoulders S_1 and S_2, the origin of which will be discussed in the next subsection.

Along the [001] azimuth the bulk Γ and X points are equivalent to the surface $\bar{\Gamma}$ points with the $\bar{X}'$ point of the surface Brillouin zone lying halfway between Γ and X. This fact may introduce surface umklapp from X to Γ, i.e., the final state lies not at Γ but at X. To study this possibility, we show in Fig. 5(a) the ARCIS spectra at the

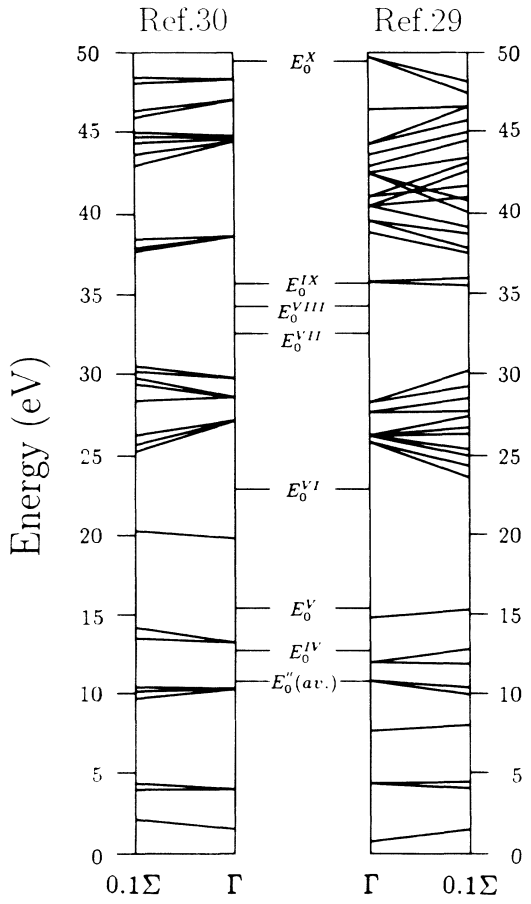

FIG. 4. Comparison of the energies of features labeled E_0 with the theoretical calculations from Refs. 29 and 30. Shown are the band structures between Γ and 10% of the Γ-K-X distance (0.1Σ). The bands in this small region are represented as straight lines for simplicity.

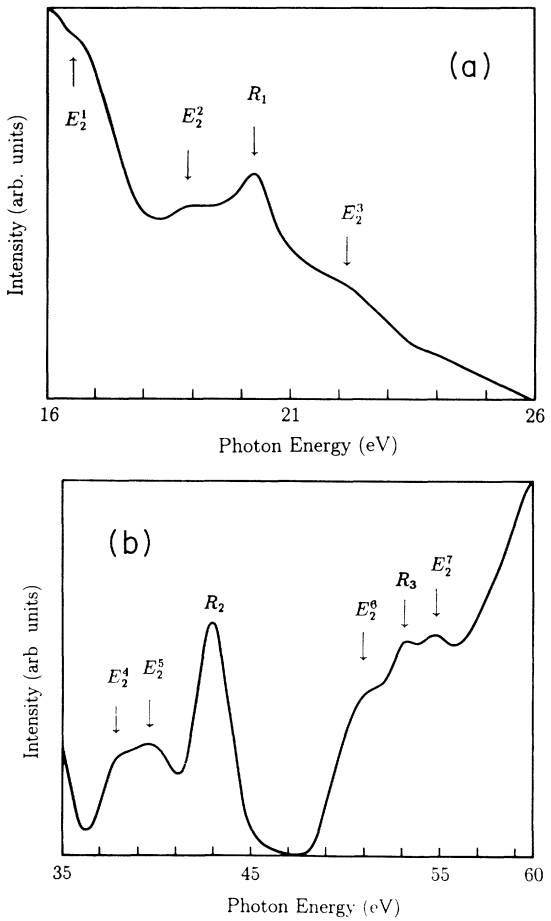

FIG. 5. Normal-emission constant-initial-state spectra from the X_3^v point ($\varepsilon_i = 6.50$ eV below the VBM). Features tentatively assigned to critical points are referred to as E_2^m. m varies between 1 and 7. (a) The photon energy ranges from 16 to 26 eV and the resonance R_1 is identified. (b) The photon energy ranges from 35 to 60 eV. Resonances R_2 and R_3 are identified.

X point selecting X_3^v at 6.50 eV below the VBM as the initial state. We find features at 10.16 eV (E_2^1) and 12.56 eV (E_2^2) and a broad structure at 15.70 eV (E_2^3), all energies above the VBM. The last feature lies close in energy to E_0^V (15.20 eV), but since E_0^V is seen also for a different azimuthal geometry,[15] for which this umklapp process is not possible, we assume that E_0^V is a conduction-band point at Γ as predicted by Ref. 29. The feature E_2^2 from Fig. 5(a) has nearly the same energy as E_0^{IV}, and according to Ref. 30 there is an available band at this energy at X. We conclude that surface umklapp between Γ and X could contribute to the primary cone emission from X and Γ, respectively.

In general, neither of the calculations agrees with the experimental energies for the higher-energy features E_0^{VI} to E_0^X observed in the present experiment. E_0^{VI} and at the close lying triplet E_0^{VII}, E_0^{VIII}, and E_0^{IX}, might be identified with a similar arrangement if we shift theoretical bands from Ref. 30 up to about 5 eV. A corresponding arrangement of levels cannot be identified in Ref. 30. Adopting this energy shift, E_0^{VII}, E_0^{VIII}, and E_0^{IX} agree with the general trend of an increasing number of bands at Γ in this energy region. Feature E_2^5 in Fig. 5(b) ($\hbar\omega = 39.36$ or 32.86 eV above the VBM) is very close in energy to E_0^{VII}. As pointed out above for features E_2^2 and E_0^{IV}, also in this case final states at X or Γ or both might contribute to E_0^{VII} and E_2^5 via surface umklapp. The theoretical band-structure predictions do not allow us to decide this question. Further features in Fig. 5(b): E_2^4 (31.32 eV above the VBM), E_2^6 (44.14 eV above the VBM), and E_2^7 (48.37 eV above the VBM) are tentatively identified as final states at the X point. Feature E_0^X agrees with both calculations but this fact may not be significant since the theoretical bands had to be shifted by about 5 eV to agree with features E_0^{VII-IX}. Peaks E_0^{XI} and E_0^{XII} are not identified in the band structures.

We conclude that both band structures are approximately correct for energies below 15 eV. This is expected for the calculations from Refs. 29 and 30 since the validity range is approximately the same as that for the valence band. Above 15 eV the differences between theory and experiment are of the same order for Ref. 29 as that of Ref. 30.

B. *S* features

Before analyzing the less prominent features labeled S, we consider the role of both inelastic scattering due to plasmon losses and Auger decay as possible contributors to the measured spectra.

The plasmon energy associated with the collective excitation of the bulk valence-band electrons has a value of 15.8 eV.[18] In our spectra the kinetic energy of the detected electrons ranges up to 50 eV, so that inelastic scattering through plasmon loss is possible. However, for the kinetic energies at hand, the scattering probability is very low so that the contribution due to plasmons is likely to appear only as background and not as structure.[34,35]

Next we consider the influence of Auger decay on our spectra. Auger processes that involve the Ga $3d$ core levels are only possible for photon energies above the excitation threshold for the core levels of 20.30 eV (see next section). That means that there is no possibility of Auger decay for initial-state energies less than $\varepsilon_i = 20.30 - 19.23 = 1.07$ eV, where 19.23 eV is the binding energy of the Ga $3d_{5/2}$ surface core level. Thus for transitions arising from Γ_{15}^v [Figs. 1(a) and 1(b)] for which $\varepsilon_i = 0$, no Auger decay is allowed. Auger processes involving As $3d$ core levels are even more restricted since these are not possible for $\varepsilon_i \leq 43.86 - 41.48 = 2.38$ eV. Here, 43.86 eV corresponds to the excitation threshold and 41.48 eV to the binding energy of the As $3d_{5/2}$ core level.

As a consequence of the analysis carried out above, the Auger decay mechanism is only possible for transitions arising from Γ_1^v [Fig. 1(c)]. In this figure no feature associated with the decay of the Ga $3d$ core hole is present because the kinetic energy of the Auger electrons is too low to appear in this spectrum. Associated with the As $3d$ core levels, the Auger processes will operate from the resonance at 43.86 eV up to the kinetic energy of $41.48 - \Phi_T' = 41.48 - 4.25 = 37.23$ eV. This value is the maximum kinetic energy that electrons can have (electrons arising from the VBM). The corresponding photon energy (55 eV) is indicated in Fig. 1(c). In the region where the Auger process can operate, we observe four features: R_2, E_0^{VIII}, E_0^{IX}, and R_3. R_2 and R_3 are resonances and will be discussed in the next subsection. Each of these two features occurs at a single photon energy for all ε_i in Fig. 2(b). This behavior is not compatible with Auger peaks that occur at constant kinetic energy. E_0^{IX} is observed also in Fig. 1(b), where the transitions arise from Γ_{15}^v, so that it cannot arise from an Auger decay. Finally, E_0^{VIII} disperses in photon energy, as observed in Fig. 2(b), with a nonconstant value for the kinetic energy. We thus conclude that Auger processes only contribute to the background in the energy region indicated in Fig. 1(c).

Features S_1 and S_2 are found at 14.20 and 16.50 eV above the VBM, respectively. The two shoulders are not predicted by either of the theoretical calculations from Refs. 29 and 30 at the Γ point and have not been observed in Ref. 15. No contribution from the Ga $3d$ or As $3d$ core levels excited with second- or third-order light from the monochromator is present at either energy. We can also rule out a contribution from Auger decay processes since the measurements are performed at Γ_{15}^v and no structure from inelastic scattering due to plasmon loss is expected at this low kinetic energy.

Reference 30 predicts bands at the X point at 14.20, 15.0, and 17.10 eV, respectively, and Ref. 29 at 13.50, 14.0, and 16.0 eV, respectively. Because the measurements were performed along the [001] azimuth, surface umklapp is allowed, which would account for S_1 and S_2. In order to confirm this possibility, we performed measurements at the X point [Fig. 5(a)] in the energy region of interest. We observe a shoulder at 15.70 eV (E_2^3) above the VBM which could be associated with S_2. The structure related with S_1 is obscured by the resonance R_1. A different possibility from the one discussed previously is

the contribution from transitions arising from the As-derived dangling-bond surface resonance that lies just below the VBM. This contribution, albeit weak, should increase in principle for increasing value of the conduction-band density of states. From Fig. 3 we observe that for energies above E_0^{IV} more final states are available so that a corresponding structure could be observed. However, with the available theoretical calculations we cannot account for two different structures S_1 and S_2.

Although it cannot be clearly established from our measurements [Fig. 5(a)], we believe S_1 and S_2 to arise from the X point via surface umklapp as predicted theoretically. A fact that favors this argument is the absence of the shoulders S_1 and S_2 in Ref. 15 where measurements were performed under a different azimuth ($[1\bar{1}0]$) where such surface umklapp is not possible.

We next discuss feature S_3 from Fig. 1(b), which appears at an energy of 38.72 eV. At this energy there is a conduction-band critical point according to Ref. 30, but, as pointed out before for E_0^{X}, this fact may not be significant since the theoretical bands had to be shifted by approximately 5 eV to force agreement with features $E_0^{\mathrm{VII-IX}}$. To study the possibility of surface umklapp we have measured ARCIS spectra from the X point [Fig. 5(b)] in the energy range of interest. Umklapp would occur if photons of $38.72+6.50=45.22$ eV could find an available final state (6.50 eV is the binding energy of X_3^v, which was used as the initial state of the ARCIS spectrum). Since no structure is found at this photon energy in Fig. 5(b), no umklapp can be identified. We can further rule out any relationship between S_3 and the As $3d$ core level excited with second-order light, which appears in Fig. 1(b) as a strong peak close to S_3. This can be done because the energy separation between S_3 and the As $3d$ peak (2.51 eV) is larger than the spin-orbit splitting [0.71 eV (Ref. 18)] and larger than the accepted surface chemical shift [0.37 eV (Ref. 36)], and because the intensities of both features are too different. As mentioned above, no Auger process is possible here either because $\varepsilon_i=0$.

The energy difference between S_6 [Fig. 1(b)] and S_3 is approximately 15 eV, which suggests an inelastic contribution from plasmon losses. This effect should be more evident for E_0^{XII}, but any structure resulting from the subtraction of the plasmon energy would be placed at the As $3d$ peak location. If any plasmon-loss effect can be observed, it is more probable to find it associated with peaks at high kinetic energy as in this case. We thus conclude that S_3 could possibly be associated with inelastic scattering due to plasmon loss from electrons in the region of S_6.

S_4 and S_5 are the replicas of R_2 and E_0^{X}, respectively. Feature S_7 [Fig. 1(c)] will be discussed in the next subsection dedicated to resonances because of its relationship with R_3. Features S_6 and S_8 arise from transitions to regions in the conduction band where many final states are available.

C. Resonances

We next analyze the resonances R_1 [Figs. 1(a) and 5(a)], R_2, and R_3 [Figs. 1(c) and 5(b)]. The peak labeled R_1 is observed at an energy of 20.30 ± 0.20 eV for all values of ε_i [Fig. 2(a)], a characteristic behavior of resonances. This feature is associated with transitions from the Ga $3d_{5/2}$ surface core level to the surface exciton, which is associated with the Ga dangling bond.[13] Our value for the resonance energy is slightly higher than the earlier reported value of 19.65 eV [measured by means of CIS (Ref. 13)], and electron-energy-loss[7] and photoemission yield spectroscopy[6] experiments that state the resonance energy to be 19.68 eV. The intensity of R_1 is reduced because the polarization vector $\hat{a}$ is nearly perpendicular to the Ga dangling bond, as mentioned above.

To deduce the surface exciton binding energy, we subtract the resonance energy from the core-level binding energy and compare the resulting value with available data of unoccupied surface states or surface resonances above the VBM for which the excitonic process is not operating. We have measured the bulk Ga $3d_{5/2}$ binding energy to be 18.95 eV below the VBM. Since the resonance takes place at a surface atom, we shift this energy by 0.28 eV (Ref. 36) towards higher energies in order to obtain the binding energy of the surface Ga $3d_{5/2}$ ($\varepsilon_i=19.23$ eV). The surface chemical shift moves the binding energies of the III-V cations to higher binding energy and those of the anions to lower binding energies.[37] In our measurements we could not identify directly the chemical shift because of insufficient resolution. Performing the subtraction we obtain $20.30-19.23=1.07$ eV. Theoretical calculations on the unoccupied surface states and surface resonances on GaAs (Ref. 20) and inverse photoemission measurements[9] place a surface band at 2.0 eV above the VBM. Therefore, we estimate the surface exciton binding energy at approximately 0.93 eV, which is in good agreement with earlier measurements both on GaAs (Ref. 9) and GaP (Ref. 38) (0.96 eV). Skibowski *et al.*[39] quote a value for the excitonic Ga $3d$ to surface-state transition which ends 420 meV below the conduction-band minimum (CBM). Adding to this value the energy of the empty surface state (0.5 eV above the CBM) we arrive at an exciton binding energy of 0.92 eV, in perfect agreement with our measurement. These values for the surface exciton binding energy have to be considered only as approximate since the surface band at 2.0 eV shows some dispersion [about 0.3 eV (Ref. 20)].

Feature R_2 [Figs. 2(b) and 5(b)] occurs at an energy of 43.86 eV and is associated with resonant photoemission related to the As $3d$ core levels (41.48 eV binding energy for As $3d_{5/2}$ as determined in this work). The process analogous to R_1 is not possible here because no available unoccupied As-derived surface states or surface resonances exist in the conduction band below the vacuum level. The process is thus due to transitions from the bulk As $3d$ core levels to the unoccupied states in the conduction band. According to Ref. 30, there is a reasonably flat band (±0.5 eV dispersion) at an energy of approximately 3.10 eV above the VBM. Note that the width of the peak R_2 (about 2 eV) is larger than this dispersion. The excitonic energy for this transition would be approximately 0.80 eV, which is comparable to that of the surface exciton derived above (0.93 eV).

In Fig. 2(b) we observe the weak but reproducible peak

R_3 that occurs at a photon energy of 53.19±0.20 eV. This feature is found at the same photon energy for all ε_i values and is observed also in Fig. 5(b). At this energy there is no possibility of a resonance with first-order light because this energy is larger than the binding energy of the Ga and As 3*d* core levels plus the photoelectric threshold ($\Phi'_T = 4.25$ eV). However, the surface Ga $3p_{3/2}$ core level can be excited by the second-order light and the resonance energy should be interpreted as 106.40 eV. The monochromator grating used in this experiment has a maximum intensity for second-order light at about 100 eV photon energy. The Ga $3p_{3/2}$ bulk component has a binding energy of 104.0 eV.[18] The chemical shift of the Ga 3*p* core levels is to our knowledge unknown, so that we will use for our analysis the same shift as for the 3*d* levels since all core levels shift approximately by the same amount.[37] The resonance energy of 106.40 eV places the final state above the VBM and below the vacuum level. The difference between this energy and the assumed binding energy of the Ga $3p_{3/2}$ surface core level is 2.12 eV, which is slightly higher than the 2.0 eV derived for the energy of an empty surface band of the Ga $3d_{3/2}$ based resonance. However, according to Ref. 20, a Ga dangling-bond-derived unoccupied surface state or surface resonance is calculated to be about 2.6 eV above the VBM. This state has not yet been observed experimentally. Thus, in principle, the transition is energetically possible but the corresponding exciton binding energy (0.5 eV) is smaller than the value obtained for R_1 (about 0.93 eV). Associated with the 0.5 eV binding energy there is an error both because the binding energy of the Ga $3p_{3/2}$ surface core level is not accurately known and because the energy of the final band has not been determined experimentally.

We next discuss feature S_7, which appears at a photon energy of 55.71 eV. This peak disperses with ε_i so that it cannot be understood as a resonance. The kinetic energy of this feature for $\varepsilon_i = 13.25$ eV is 38.0 eV. As pointed out above, second-order light has a maximum intensity around 100 eV, so that a hole in the Ga 3*p* core level can be created with (2)55.71 = 111.42 eV photons. We thus interpret S_7 as due to an Ga 3*p* – Ga 3*d* – As 3*d* interatomic Auger decay[40] which has a nominal (neglecting final-state interactions) kinetic energy of $104 - 19 - 42 - \Phi'_T \sim 39$ eV, a value very close to the measured 38 eV. Because S_7 is weak we cannot state if the kinetic energy of S_7 is independent of ε_i, which would confirm the Auger character. The As 3*d* holes would in turn decay so that a new Auger process is expected. The allowed range for this last decay goes from R_3 up to 37.23 eV kinetic energy since the excitation can only start from R_3 and the Auger limit associated with the As 3*d* and the valence-band electrons is found at $K = 37.23$ eV, as discussed above [see Fig. 1(c)].

Feature E_2^7 has nearly the same energy as S_7 but the possibility of a resonance has been ruled out above. The fact that the energies lie so close could be fortuitous since many final bands are expected at *X* at these energies. The spin-orbit splitting of the Ga 3*p* core levels is 3.68 eV,[18] which is larger than the energy difference between R_3 and S_7, so that no such contribution is possible. We thus associate S_7 with an interatomic Auger decay.

IV. SUMMARY

We have extended the experimental determination of the conduction-band energies at the Γ point in GaAs up to approximately 60 eV by means of ARCIS spectroscopy. We have determined in this energy range ten clear features that are assigned to direct transitions arising from Γ_{15}^v (VBM) and Γ_1^v (13.25 eV below the VBM).

ARCIS is a very useful tool for determining the energy resonances from the core levels to unoccupied states above the VBM because of the constancy of the transition energy for different initial-state energy. We observe the resonances associated with Ga 3*d*, Ga 3*p*, and As 3*d* core-level excitations and derive surface exciton binding energies between 0.5 and 0.93 eV. A weak but reproducible feature is observed that is related to interatomic Auger decay between the As and Ga atoms.

ACKNOWLEDGMENTS

This work was supported by the Bundesministerium für Forschung und Technologie and by the Australian German Scientific agreement. J.F. would like to thank the Directorate General for Science, Research and Development (European Community) for financial support and (A.S.) to La Trobe University for support. Thanks are due to the staff of the Berliner Elektronenspeicherring-Gesellschaft für Synchrotronstrahlung m.b.H. (BESSY) synchrotron for their support and hospitality and to Professor Cardona for supporting the collaboration with the Max-Planck-Institut für Festkörperforschung. We also appreciate R. Denecke for helping us in the experiments.

[1] D. E. Aspnes, in *Handbook of Optical Constants of Solids*, edited by E. D. Palik (Academic, New York, 1985).
[2] T. Wegehaupt, D. Rieger, and W. Steinmann, Phys. Rev. B **37**, 10086 (1988).
[3] Y. Lassailly, P. Chiaradia, C. Hermann, and G. Lampel, Phys. Rev. B **41**, 1266 (1990).
[4] D. E. Aspnes, C. G. Olson, and D. W. Lynch, Phys. Rev. B **12**, 2527 (1975).
[5] R. L. Johnson, J. Barth, M. Cardona, D. Fuchs, and A. M. Bradshaw, Rev. Sci. Instrum. **60**, 2209 (1989).
[6] J. C. McMenamin and R. S. Bauer, J. Vac. Sci. Technol. **15**, 1262 (1978).
[7] H. Lüth, M. Büchel, R. Dorn, M. Liehr, and R. Matz, Phys. Rev. B **15**, 865 (1977).
[8] P. Mårtensson, A. Cricenti, and G. V. Hansson, Phys. Rev. B **33**, 8855 (1986).
[9] D. Straub, M. Skibowski, and F. J. Himpsel, Phys. Rev. B **32**, 5237 (1985).

[10]G. J. Lapeyre, A. D. Baer, J. Hermanson, J. Anderson, J. A. Knapp, and P. L. Gobby, Solid State Commun. **15**, 1601 (1974).
[11]A. Bianconi, S. B. M. Hagström, and R. Z. Bachrach, Phys. Rev. B **16**, 5543 (1977).
[12]G. J. Lapeyre, R. J. Smith, and J. Anderson, J. Vac. Sci. Technol. **14**, 384 (1977).
[13]G. J. Lapeyre and J. Anderson, Phys. Rev. Lett. **35**, 117 (1975).
[14]L. Ley, M. Taniguchi, J. Ghijsen, R. L. Johnson, and A. Fujimori, Phys. Rev. B **35**, 2839 (1987).
[15]J. A. Knapp and G. J. Lapeyre, Il Nuovo Cimento B **39**, 693 (1977).
[16]J. Fraxedas, H. J. Trodahl, and L. Ley, Phys. Scr. **41**, 905 (1990).
[17]R. C. G. Leckey and J. R. Riley, Appl. Surf. Sci. **22/23**, 196 (1985).
[18]*Electronic Structure of Solids: Photoemission Spectra and Related Data,* Vol. 23 of *Landolt-Börnstein: Functional Relationships in Science and Technology,* edited by A. Goldmann and E. E. Koch (Springer, Berlin, 1989).
[19]Unpublished.
[20]C. Mailhiot, C. B. Duke, and D. J. Chadi, Phys. Rev. B **31**, 2213 (1985).
[21]J. van Laar, A. Huijser, and T. L. van Rooy, J. Vac. Sci. Technol. **14**, 894 (1977).
[22]J. Fraxedas, M. Kelly, and M. Cardona, unpublished; J. Fraxedas, H.J. Trodahl, S. Gopalan, L. Ley, and M. Cardona, Phys. Rev. B **41**, 10 068 (1990).
[23]G. P. Williams, R. J. Smith, and G. J. Lapeyre, J. Vac. Sci. Technol. **15**, 1249 (1978).
[24]M. Cardona, N. E. Christensen, and G. Fasol, Phys. Rev. B **38**, 1806 (1988).
[25]G. P. Williams, F. Cerrina, G. J. Lapeyre, J. R. Anderson, R. J. Smith, and J. Hermansson, Phys. Rev. B **34**, 5548 (1986).
[26]K. A. Mills, D. Denley, P. Perfetti, and D. A. Shirley, Solid State Commun. **30**, 743 (1979).
[27]For a discussion on the determination of VBM, see H. Höchst, D. Niles, and I. Hernández-Calderón, Phys. Rev. B **40**, 8370 (1989).
[28]D. E. Aspnes and A. A. Studna, Phys. Rev. B **7**, 2940 (1973).
[29]J. Koukal, private communication.
[30]The theoretical conduction bands of Ref. 24 are extended in our present work up to 50 eV to permit the comparison with the experimental data.
[31]K. C. Pandey and J. C. Phillips, Phys. Rev. B **9**, 1552 (1974).
[32]J. R. Chelikowski, T. J. Wagener, J. H. Weaver, and A. Jin, Phys. Rev. B **40**, 9644 (1989).
[33]J. Fraxedas, S. Zollner, A. Stampfl, R. C. G. Leckey, J. D. Riley, and L. Ley, unpublished.
[34]R. C. G. Leckey, Solid State Commun. **10**, 971 (1972).
[35]J. E. Inglesfield, J. Phys. C **16**, 403 (1983).
[36]D. E. Eastman, F. J. Himpsel, and J. F. van der Veen, J. Vac. Sci. Technol. **20**, 609 (1982).
[37]V. Hinkel, L. Sorba, and K. Horn, Surf. Sci. **194**, 597 (1988).
[38]D. Straub, M. Skibowski, and F. J. Himpsel, J. Vac. Sci. Technol. A **3**, 1484 (1985).
[39]M. Skibowski, G. Sprüssel, and V. Saile, Appl. Opt. **19**, 3978 (1980).
[40]M. L. Knotek and P. J. Feibelman, Phys. Rev. Lett. **40**, 964 (1978).